Probability distribution of bed particle instability

Cheng, Nian-Sheng; Law, Adrian Wing-Keung; Lim, Siow Yong.

2003

Cheng, N. S., Law, A. W. K. & Lim, S. Y. (2003). Probability distribution of bed particle instability. Advances in Water Resources, 26(4), 427-433.

https://hdl.handle.net/10356/94194

https://doi.org/10.1016/S0309-1708(02)00184-7

Probability distribution of bed particle instability

Nian-Sheng Cheng*, Adrian Wing-Keung Law and Siow Yong Lim

School of Civil and Environmental Engineering, Nanyang Technological University

Nanyang Avenue, Singapore 639798

Abstract

The probability distribution of the instability of bed particles is essential for application of statistical approaches to describe bedload transport. The instability generally depends on the near-bed flow conditions and characteristics of the particle packing on the bed surface. In this study, only irregularity of the bed particles is considered. The instability of each individual bed particle is characterised using an effective shear stress, beyond which the particle starts to move. The effective shear stresses vary randomly over the bed because of the randomness of the bed particles. For a flat bed comprised of uniform particles, the variation is demonstrated to be a narrow-banded random process with amplitudes equal to the magnitudes of the effective shear stress. A theoretical derivation shows that the probability density distribution of the effective shear stress follows the Rayleigh distribution. Subsequent analysis also indicates that the probability of the instability is proportional to the square of the bed shear stress for low rates of bedload transport.

Keywords: bedload transport, probability, bed shear stress, Rayleigh distribution, critical shear stress, instability

* Corresponding author. Tel.: 65-6790-6936; fax: 65-6791-0676. Email: cnscheng@ntu.edu.sg

1. Introduction

Bedload transport includes a number of probabilistic events of the bed particle movement and is closely related to the statistical characteristics of flow and bed particle configuration. To utilize a stochastic method to compute bedload transport rates, a major problem is to evaluate the probability characteristics of bed particle instability. This was often ignored in many previous studies (e.g., Einstein 1950).

Generally, the bed particles may perform rolling, sliding or saltating motions depending on flow and bed conditions. When the sediment bed is strongly influenced by turbulence, for example, in the case of hydraulically rough beds, saltation may be the main mode in which the particles are detached from their positions of rest. Then, it is reasonable to define the probability of the bed instability as that of the hydrodynamic lift force exerted on a particle greater than its submerged weight. The probability distribution of the instability can then be derived if the statistical properties of the lift or the near-bed turbulence velocity are known. With the assumption that the lift follows the Gaussian distribution, Einstein (1950) derived a theoretical expression for the probability of erosion, leading to his well-known bedload function for equilibrium sediment beds. However, Einstein did not consider explicitly the effect of the bed randomness on the probability of erosion. It is also noted that the probability density function of the lift must be non-Gaussian if the near-bed velocity is assumed to distribute in the Gaussian fashion (Cheng and Chiew 1998).

By comparison, for laminar flows or even hydraulically smooth beds, bed particles are predominantly subjected to viscous shear rather than turbulent disturbances. Viscous shear may prevail in the longitudinal flow direction in comparison with turbulence eddies

which can attack the bed at various angles. Therefore, bed particles in laminar flows are expected to move largely in rolling and sliding modes. This implies that in addition to the lift, F_L, and submerged weight, W, the drag parallel to the flow, F_D, should also be included to define the condition for a particle to roll or slide over others.

For the case of hydraulically rough beds, the randomness of the particle instability varies depending on the turbulence fluctuations at the bed surface. In the presence of predominantly viscous shear, the random arrangement of the bed particles may have more significant effects on the statistical characteristics of the bed instability than those caused by the near-bed flow variation.

Various particle arrangements exist even for flat bed conditions, because a bed particle can differ from its neighbours in size, shape and position. To quantify the randomness of a bed comprised of uniform particles, a useful approach is to introduce the concept of exposure of the particles (Paintal 1971). As shown in Fig. 1, the exposure, e, is defined as the protrusion of a particle above the mean bed level. The dimensionless exposure parameter can then be taken as the ratio of e to the particle diameter, e/D. Note that other factors such as hiding effects should also be taken into consideration for non-uniform particles (Parker 1990).

Since particles are randomly positioned on the bed, different particles have different exposure to the flow. A particle with higher exposure than that of its neighbours is subjected to larger hydrodynamic forces. Furthermore, a particle with higher exposure with respect to its immediate downstream neighbour can be detached at a relatively smaller angle, β, as shown in Fig. 1. β is called the angle of escape and defined as the angle of a plane along which the particle is supposed to be detached (Paintal 1971).

Generally, whether a particle will move depends on β and the relevant hydrodynamic forces on the particle. There are two limiting cases for the escape: $\beta = 0$ and $\beta = 90^o$. As shown in Fig. 2, the former represents the case of the maximum exposure, i.e., $e/D = 1$, and correspondingly the minimum bed shear stress to initiate movement of the particle is almost zero. On the other hand, $\beta = 90^o$ represents the case when the exposure of the particle is the same as that of its downstream neighbour. The minimum bed shear stress for the particle to move hence approaches infinity if the submerged weight of the particle W is greater than the lift F_L. Note that the condition $W < F_L$ implies that the particle can be lifted up, moving probably in the saltating mode. For simplicity, we assume that the particles would move mainly in the rolling mode once they are detached from their positions of rest. Therefore, the critical condition can be mathematically expressed as

$$\frac{F_D}{W - F_L} > tan\,\beta \tag{1}$$

Obviously, for particles moving in the rolling mode, it is reasonable to use Eq. (1) for defining the probability of the instability. Such a definition can be substantiated only when F_L, F_D, and β are known. To evaluate these parameters, for example, Paintal (1971) assumed that the particle exposure was uniformly distributed, and both F_L and F_D had the same maximum values and were proportional to the relative exposure of the particle with respect to its downstream neighbour. These assumptions were made without verifications and thus may not be realistic. The study conducted by He and Han (1982), who proposed a stochastic model for incipient sediment motion, is similar to Paintal's work but subjected to different assumptions. The probabilistic nature of the near-bed flow was also addressed earlier by Gessler (1970) in investigating the bed self-stabilizing process. However, the bed randomness was ignored in his consideration.

The utilisation of the hydrodynamic forces induced by the near-bed flow in studying the stability of bed particles is conceptually straightforward. However, the difficulty in such approaches is the determination of the lift and drag coefficients because prediction of the near-bed flow in the presence of the bed particles remains an intractable problem. Grass (1970) considered that the initial bed instability can be defined in terms of parameters which represent intrinsic properties of the bed material and are independent of the near-bed flow conditions. He further identified two kinds of shear stress distributions in exploring the initial instability of fine sand. One is the critical shear stress distribution associated with the bed material, while the other is the shear stress distribution applied to the bed by the particular flow. He suggested that the initial motion of sediment results when the most susceptible particles, those with the lowest characteristic critical shear stresses, are subjected to the highest shear stresses applied by the ambient flow. Grass used a 250-frame per second camera to photograph simultaneously the bed sand grains and hydrogen bubble tracers. By identifying the frames where unstable particles were recorded, the corresponding instantaneous characteristic critical shear stresses were then determined from the viscous sublayer velocity profile shown by the hydrogen bubble tracers. Unfortunately, the statistical results of the experimental data yield no clear distributions for the characteristic critical shear stress, perhaps because the sample size was limited to only 25 unstable grains for each experiment.

In this study, the concept of the characteristic critical shear stress by Grass (1970) is used to describe the instability of individual bed particles. For convenience, we use the term “effective shear stress” to differentiate from the critical shear stress that is usually associated with the Shields diagram. Compared to the Shields shear stress that is for the “average” initiation of bed particles, the effective shear stress is taken as a random variable. The analysis presented in this paper is largely limited to the case of a flat bed

comprised of uniform particles. This ensures that the randomness of the effective shear stress is simplified allowing the probability distribution of the bed particle instability to be explored analytically.

2. Theoretical Derivation

Consider the minimum shear stress required for a bed particle to move, which is referred to as the effective shear stress, τ_e, in this study. As discussed previously, τ_e is a random variable and has two extreme values, i.e., $\tau_e \to 0$ and $\tau_e \to \infty$, corresponding to β = 0 and $\beta = 90^o$, respectively (see Fig. 2). Assuming that the probability density function of τ_e is $f(\tau_e)$, the probability of bed particle instability can simply be defined as

$$p = p(\tau_e < \tau) = \int_o^\tau f(\tau_e) d\tau_e \tag{2}$$

where τ = bed shear stress exerted by the flow.

First, consider a regular arrangement of bed particles, as shown in Fig. 3, where the surface particles consist of group A and group B and the difference in elevation between the two layers is Z_{AB}. Obviously, the effective shear stress for group A, τ_{eA}, is much smaller than that for group B, τ_{eB}, and the difference between them is equal to zero if Z_{AB} = 0, and approaches infinity if $Z_{AB} = D$. Corresponding to the different positions of the particles, the effective shear stress in the horizontal direction (or x-direction) undulates in a regular fashion.

In reality, the bed particles are randomly distributed and the τ_e-distribution must be irregular as sketched in Fig. 4. As mentioned earlier, the irregularity is generally due to the

randomness of bed particle configurations. For the case of a flat bed comprised of uniform particles, the geometrical distribution of the bed particles on the bed surface plane is statistically independent of direction. Two aspects can be observed. First, the magnitude of the effective shear stress depends on the exposure of the particle, the higher the exposure the lower the effective shear stress. Second, the distribution of τ_e over the bed is associated with locations of various particles within the surface layer. The locations can further be characterised with a series of distances between neighbouring particles in a certain direction on the bed. The latter is referred to as the step length, L, as shown in Fig. 5. The finer the particles, the more frequent the changes in the effective shear stress. For the case where the bed particles are uniformly sized, the frequency of the variation along the bed is expected to be narrow-banded. Further explanations for this consideration are given in the following.

The particles in the bed surface layer can generally be taken as those packed near the mean bed level, of which the centres are confined in a region of approximately one diameter in thickness. For simplicity, we first consider a two-dimensional bed particle configuration as shown in Fig. 5. The horizontal distance, L, between the centres for any two neighbouring particles within the surface layer can be equal to or smaller than the particle diameter if they are in contact with each other, as shown in Fig. 5(a). Otherwise, L can be greater than the particle diameter as shown in Fig. 5(b) if there is a gap between the two particles. This gap should not be more than $2D$ so that no other surface particles can appear between them. Therefore, it is reasonable to assume that the horizontal distance which occurs most frequently is equal to approximately the particle diameter. Though the particle arrangement shown in Fig. 5 is only two-dimensional, the assumption made is found to be consistent with experimental observations conducted in this study for a three-dimensional bed configuration.

2.1. Experiment

The experiment was conducted to investigate directly the distribution of the distance between particles on the bed surface. First, a sediment bed was prepared using uniformly sized marbles of 15 mm in diameter. It is noted that the size of the marble should not have effects on the probability distribution of L/D. The marbles were randomly packed, but providing a generally flat bed surface. The bed surface was then photographed using a digital camera. The location of each surface particle was subsequently determined by its corresponding central pixel in the particle image. The pixel size was approximately 4% of the diameter of the marbles. Next, the image was superimposed with a grid comprised of two families of parallel lines, which were perpendicular to each other. Along each straight line, a strip with a width of one diameter of the marble was first defined, and the marbles whose centres were confined within the strip were then identified. All distances between two neighbouring marbles were then measured in the direction parallel to the line. In this manner, a series of data of the abovementioned distance, L, were generated, of which a sample is plotted in Fig. 6. It shows that L varies randomly from particle to particle, but being generally less than $2D$. The probability density function of the distance was subsequently computed, as shown in Fig. 7, indicating that the distance which occurred most frequently is approximately equal to the diameter of the marbles.

2.2. Probability density function, $f(\tau_e)$

With the above considerations, the probability distribution of the effective shear stress can be analysed based on a hypothetical random wave process, of which the amplitude is taken as $\tau_e/2$ and the wave length is L, as shown in Fig. 8. It should be noted that the main concern in this study is the distribution of the wave amplitude for the

hypothetical process. If the random wave process is assumed to be comprised of a large number of sinusoids, it can be expressed as:

$$\eta(x) = \sum_{i=1}^{\infty} a_i \cos(k_i x - \varepsilon_i) \tag{3}$$

and an equivalent expression in complex notation is

$$\eta(x) = \mathrm{Re}\left(\sum_{m=1}^{\infty} a_m e^{i(k_m x - \varepsilon_m)} \right) \tag{4}$$

where a_i = amplitude, k_i = wave number, ε_i = random phase and Re refers to the real component.

As implied by Fig. 7, the wave numbers for all the components of the process can be further considered to be near a common value, k_p, corresponding to the average wave length, $L = D$, i.e. $k_p = 2\pi/D$. To estimate the relevant spectral width, the probability density function obtained from the experiment can be fitted to the following formula:

$$f(t) = \left(\frac{v}{t}\right)^2 \frac{1}{1 + \frac{1}{\sqrt{1+v^2}}} \frac{1}{\left[v^2 + \left(1 - \frac{1}{t}\right)^2 \right]^{1.5}} \tag{5}$$

where $t = L/D$ and v = bandwidth parameter. Eq. (5) can be derived using the Longuet-Higgins distribution, which is applicable to a narrow spectrum when the bandwidth parameter $v < 0.6$ (Massel, 1998). Fig. 7 shows that the computed probability density function can be represented by (5) for $v = 0.4$. This result indicates that the hypothetical random process is almost narrow-banded.

Using the wave number, k_p, (4) can be rewritten as

$$\eta(x) = Re\left(A e^{i\varphi} e^{ik_p x} \right) \tag{6}$$

where A and φ are real functions of x, and

$$Ae^{i\varphi} = \sum_{m=1}^{\infty} a_m e^{i\left[(k_m - k_p)x - \varepsilon_m\right]} \tag{7}$$

If $|k_m\text{-}k_p|$ is much smaller than k_p, $Ae^{i\varphi}$ varies slowly compared to the process $\eta(x)$ and serves as an envelope of the process. Therefore, the probability distribution of the wave amplitude can be obtained only by examining the statistics of $Ae^{i\varphi}$.

From statistical theory, it can be shown that the probability density of the wave amplitude A follows the so-called Rayleigh distribution (see Appendix), i.e.

$$f(A) = \frac{A}{\mu_o} exp\left(-\frac{A^2}{2\mu_o}\right) \tag{8}$$

where $\mu_o = \overline{\eta^2}$. Since $A = \tau_e/2$, the Jacobian $|d\tau_e/dA| = 2$ and

$$A_{rms} = \frac{\tau_{erms}}{2} = \sqrt{\int_0^{\infty} A^2 f(A) dA} = \sqrt{2\mu_o} \tag{9}$$

where the subscript rms refers to taking the root-mean-square values, the probability density function of τ_e can be derived using (8) as follows:

$$f(\tau_e) = \frac{2\tau_e}{\tau_{erms}^2} exp\left(-\frac{\tau_e^2}{\tau_{erms}^2}\right) \tag{10}$$

In addition, since the average value of the effective shear stress can be related to its rms value in the form

$$\overline{\tau_e} = \int_0^{\infty} \tau_e f(\tau_e) d\tau_e = \frac{\sqrt{\pi}}{2} \tau_{erms} \tag{11}$$

(10) can also be expressed as

$$f(\tau_e) = \frac{2\tau_e}{\tau_{erms}^2} exp\left[-\left(\frac{\tau_e}{\tau_{erms}}\right)^2\right] = \frac{\pi}{2}\frac{\tau_e}{\overline{\tau_e}^2} exp\left[-\frac{\pi}{4}\left(\frac{\tau_e}{\overline{\tau_e}}\right)^2\right] \tag{12}$$

2.3. Probability of bed particle instability

As is defined by (2) and sketched in Fig. 9, the probability of the bed particle instability can be computed by integrating (12) with respect to τ_e from $\tau_e = 0$ to $\tau_e = \tau$:

$$p = \int_o^{\tau} f(\tau_e) d\tau_e = 1 - exp\left[-\frac{\pi}{4} \left(\frac{\tau}{\overline{\tau_e}} \right)^2 \right] \tag{13}$$

Eq. (13) is plotted in Fig. 10, showing that the probability increases with increasing ratio of the bed shear stress to the effective shear stress.

3. Discussion

Eq. (13) can be evaluated only when the average effective shear stress $\overline{\tau_e}$ is known. However, general information on $\overline{\tau_e}$ is not available in the literature. As an approach for evaluating the average bed particle instability, $\overline{\tau_e}$ can be related to the critical shear stress, τ_c, that can be computed using the Shields diagram. The difference is that $\overline{\tau_e}$ is concerned with the instability with more bed particles than those implied by τ_c. When $\tau = \overline{\tau_e}$, (13) gives a value of p = 54%, indicating that slightly more than half of the particles on the bed are in motion. In comparison, much fewer particles are assumed to be in motion when $\tau = \tau_c$. For example, the so-called qualitative criterion, "weak movement", and some small dimensionless transport rates are often used to define the condition of the incipient sediment motion (Lavelle and Mofjeld 1987). In the case of hydraulically rough beds, Cheng and Chiew (1998) reported that the probability of erosion is equal to approximately 0.6% for the incipient condition. Using the same condition of p = 0.6%, one can obtain from (13) that $\tau_c = 0.09\overline{\tau_e}$, showing that the critical shear stress is at least one order of magnitude smaller than the average effective shear stress.

Furthermore, for very small values of bed shear stresses, Eq. (13) can be simplified through a series expansion of the exponential function to:

$$p = \frac{\pi}{4}\left(\frac{\tau}{\overline{\tau_e}}\right)^2 \tag{14}$$

As shown in Fig. 10, Eq. (13) and Eq. (14) are very close if the applied shear stress is less than approximately 50% of the average effective shear stress. Eq. (14) shows that the probability of the bed particle instability is proportional to the square of the bed shear stress for small bed shear stresses or low sediment transport rates.

The above considerations include no effects of the near-bed flow variations. This means that Eq. (13) and Eq. (14) are only applicable for the case of uniform bed shear stresses. However, if the bed shear stress varies from τ_{min} to τ_{max} with a known probability density function $f(\tau)$, then Eq. (13) can be generalised as

$$p = \int_{\tau_{min}}^{\tau_{max}} f(\tau)\int_{o}^{\tau} f(\tau_e)d\tau_e d\tau = \int_{\tau_{min}}^{\tau_{max}} f(\tau)\left[1 - exp\left(-\frac{\pi}{4}\frac{\tau^2}{\overline{\tau_e}^2}\right)\right]d\tau \tag{15}$$

In order to use Eq. (15) to evaluate the probability of the bed particle instability, further studies are needed to determine the average effective shear stress and the probability density function of the bed shear stress exerted by the flow.

Since the present derivation is conducted only for uniform bed particles, the theory should be modified when applied to cases where non-uniform sediment is presented. This may be done by further incorporating other relevant factors such hiding effects.

4. Conclusions

In this paper, the instability of each individual bed particle is analysed in terms of its own effective shear stresses. For the case of uniform sediment particles, the variation of the effective shear stress is shown to be a narrow-banded wave process. This leads to that the effective shear stress varies in accordance with the Rayleigh distribution. The result indicates that the average effective shear stress refers to the condition such that slightly more than half of the particles on the bed are in motion. The analysis also shows that the probability of the bed particle instability is proportional to the square of the bed shear stress for low sediment transport rates.

Appendix: The probability density function of the amplitude A.

The subsequent derivation is conducted using similar approaches previously applied to statistics of radiowaves (Garg and Wilkes 1996) and ocean waves (Longuet-Higgins 1952; Massel 1998).

From Eq. (6), the wave process $\eta(x)$ can be rewritten as

$$\eta(x) = A_c(x)\cos(k_p x) - A_s(x)\sin(k_p x) \tag{16}$$

where

$$A_c(x) = \sum_{m=1}^{\infty} a_m \cos\left[\left(k_m - k_p\right)x - \varepsilon_m\right] \tag{17}$$

$$A_s(x) = \sum_{m=1}^{\infty} a_m \sin\left[\left(k_m - k_p\right)x - \varepsilon_m\right] \tag{18}$$

Since the wave process is narrow-banded, the amplitude $A_c(x)$ and $A_s(x)$ vary slowly compared to $\eta(x)$. Furthermore, let

$$A_c(x) = A(x)\cos\varphi(x) \tag{19}$$

$$A_s(x) = A(x)\sin\varphi(x) \tag{20}$$

where

$$A(x) = \sqrt{A_c^2(x) + A_s^2(x)} \tag{21}$$

$$\varphi(x) = \tan^{-1}[A_s(x)/A_c(x)] \tag{22}$$

This leads to that Eq. (16) can be further expressed in terms of amplitude $A(x)$ and phase $\varphi(x)$ as follows:

$$\eta(x) = A(x)\cos[k_p x + \varphi(x)] \tag{23}$$

As mentioned earlier, the amplitude A is equal to the amplitude of the wave envelope, which varies slowly in x. According to the Central Limit Theorem, A_c and A_s follow the Gaussian distribution with mean value equal to zero and variance μ_o given as

$$\mu_o = E[A_c^2] = E[A_s^2] = E[\eta^2] \tag{24}$$

It can also be shown that $E[A_cA_s] = 0$. Therefore, the joint probability density function can be obtained as:

$$f(A_c, A_s) = f(A_c)\,f(A_s) = \frac{1}{2\pi\mu_o}\exp\left(-\frac{A_c^2 + A_s^2}{2\mu_o}\right) \tag{25}$$

Using Eq. (25) and the Jacobian of the variable transformation:

$$J = \frac{\partial(A_c, A_s)}{\partial(A, \varphi)} = A \tag{26}$$

we obtain the following joint probability density distribution:

$$f(A, \varphi) = J \cdot f[A_c(A, \varphi),\, A_s(A, \varphi)] = \frac{A}{2\pi\mu_o}\exp\left(-\frac{A^2}{2\mu_o}\right) \tag{27}$$

Integrating Eq. (27) with respect to φ from 0 to 2π yields

$$f(A) = \frac{A}{\mu_o} exp\left(-\frac{A^2}{2\mu_o}\right) \tag{28}$$

Eq. (28) shows that the probability density distribution of the amplitude A can be described using the well-known Rayleigh function.

References

[1] Cheng NS and Chiew YM. Pickup probability for sediment entrainment. J Hydr Eng ASCE 1998; 4(2): 232-235.

[2] Einstein HA. The bed-load function for sedimentation in open channel flows. In *Sedimentation*, edited and published by Shen HW, Colorado State University, Fort Collins, Colorado, USA. 1950.

[3] Grass AJ. Initial instability of a fine bed sand. J Hydr Div ASCE 1970; 96(3): 619-631.

[4] Garg VK and Wilkes JE. *Wireless and Personal Communications Systems.* Prentice-Hall Inc., USA, 1996.

[5] Gessler J. Self-stabilizing tendencies of alluvial channels. J Waterways and Harbours Div ASCE 1970; 96(2):235-249.

[6] He M and Han Q. Stochastic model of incipient sediment motion. J Hydr Div ASCE 1982; 108(2): 211-224.

[7] Lavelle JW and Mofjeld HO. Do critical stresses for incipient motion and erosion really exist? J. Hydr Div ASCE 1987; 113(3): 370-385.

[8] Longuet-Higgins MS. On the statistical distribution of heights of sea waves. J Mar Res 1952; 11: 245-266.

[9] Massel SR. *Ocean surface waves: their physics and prediction*. World Scientific Publishing Co Pte Ltd, Singapore, 1998.

[10] Paintal AS. A stochastic model of bed load transport. J Hydr Res 1971; 9(4): 527-554.

[11] Parker G. Surface-based bedload transport relation for gravel rivers. J Hydr Res 1990; 28(4):417-436.

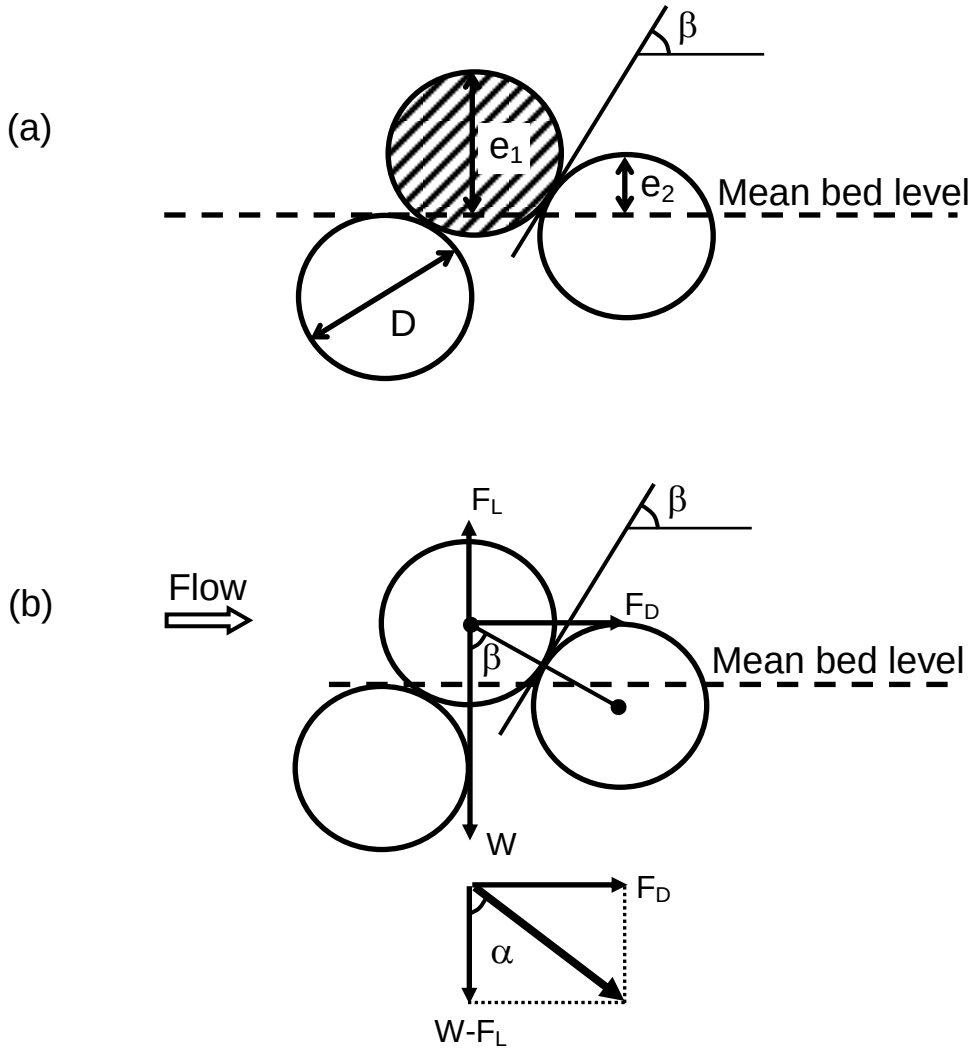

Fig. 1. Exposure of Surface Particles and Forces Exerted by Flow

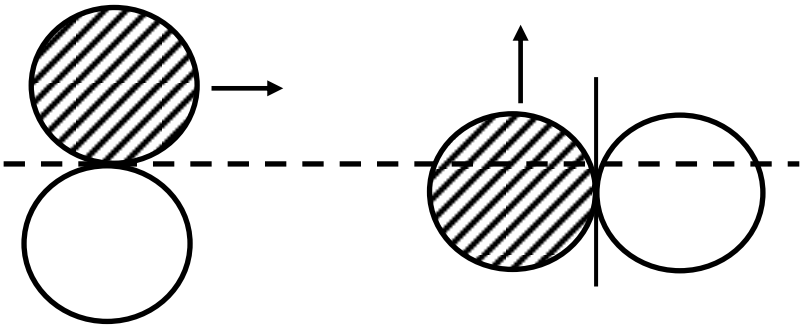

$\beta = 0$
$\tan\beta = 0$
$\tau_e \rightarrow 0$

$\beta = 90^o$
$\tan\beta = \infty$
$\tau_e \rightarrow \infty$

Fig. 2. Two Extreme Cases of Surface Particles

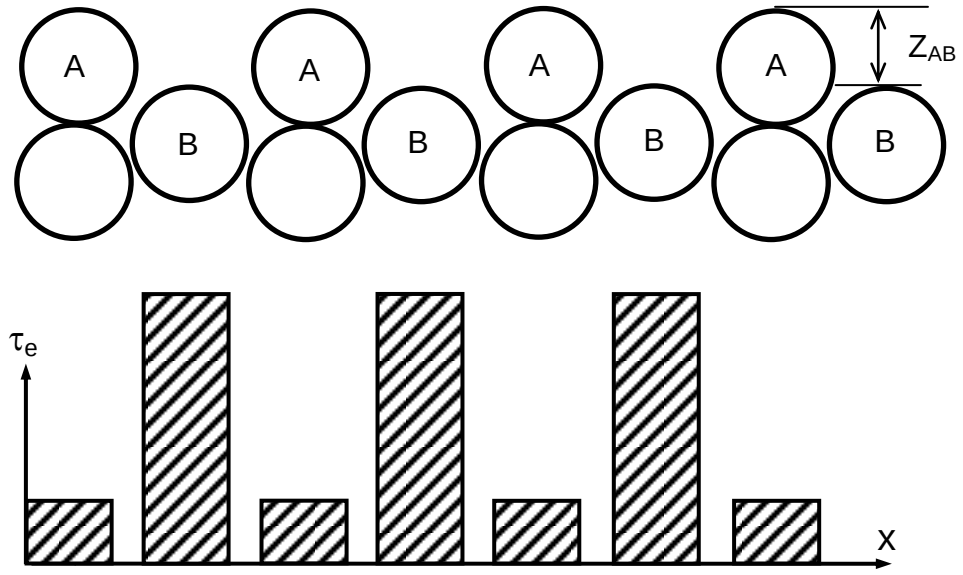

Fig. 3. Effective Shear Stress Distribution for a Simple Bed Configuration

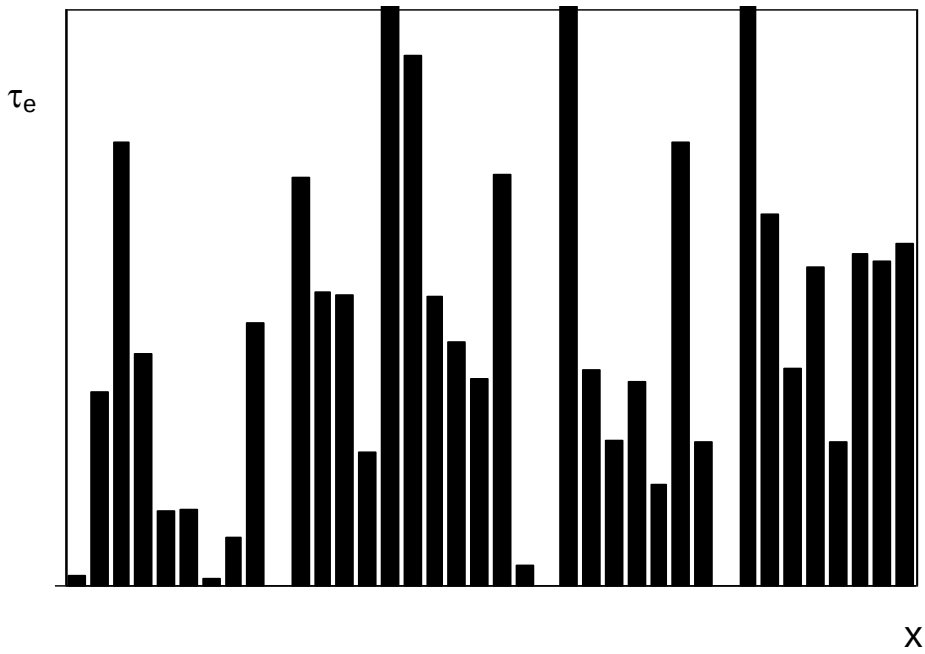

Fig. 4. Sketch of Random Distribution of Effective Shear Stress

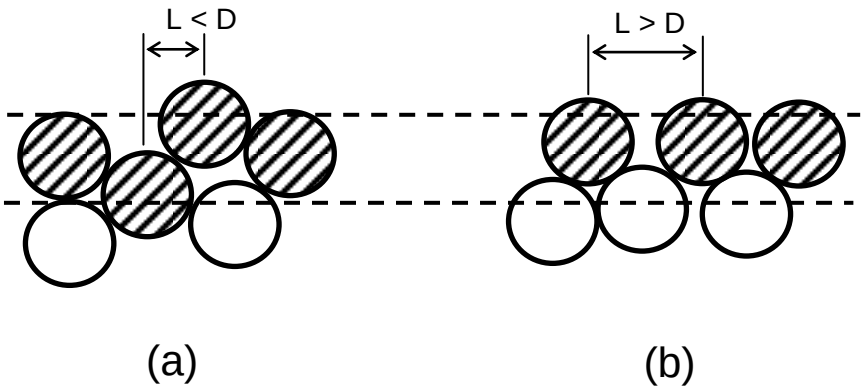

Fig. 5. Distance between Two Neighbouring Surface Particles

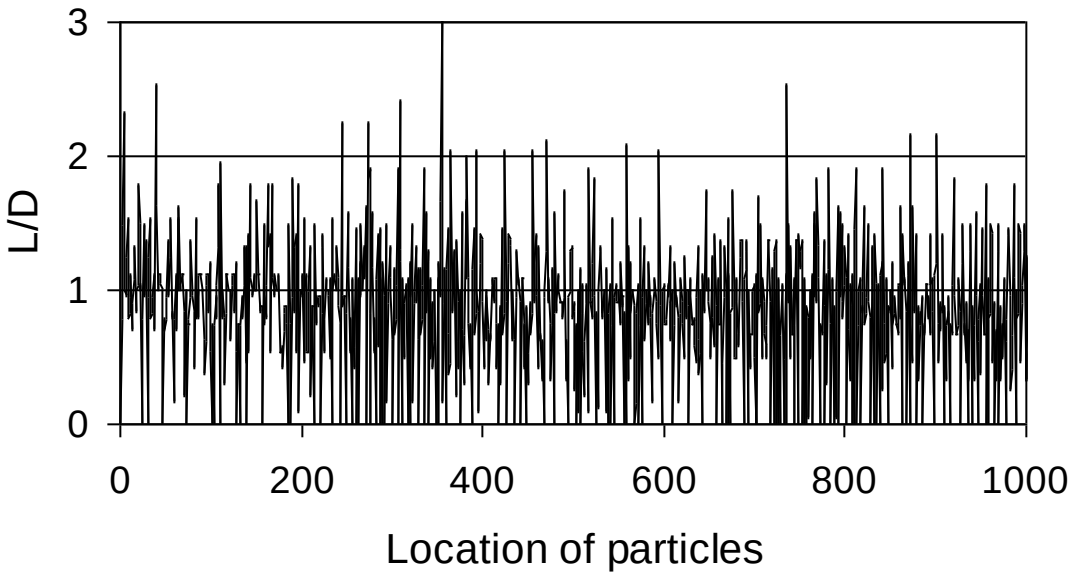

Fig. 6. Measurements of Distance between Two Neighbouring Marbles

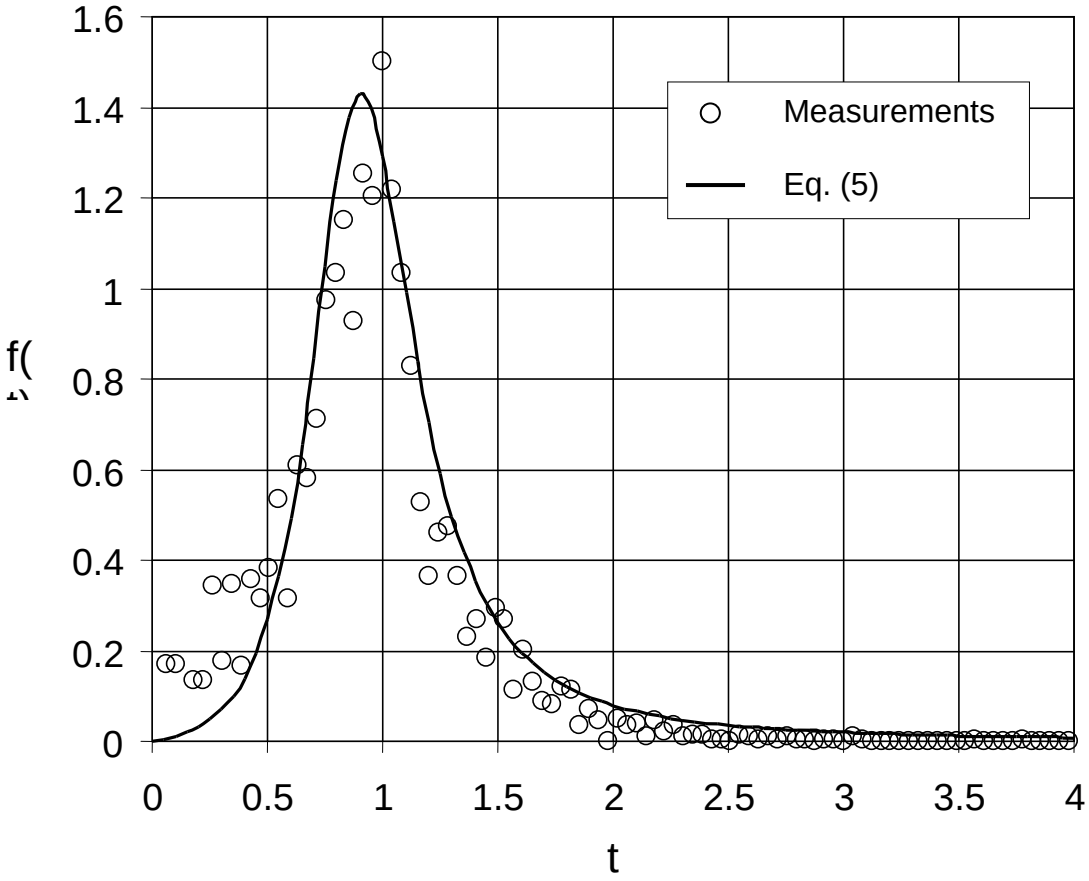

Fig. 7. Probability Density Distribution of Normalised Distance, t = L/D

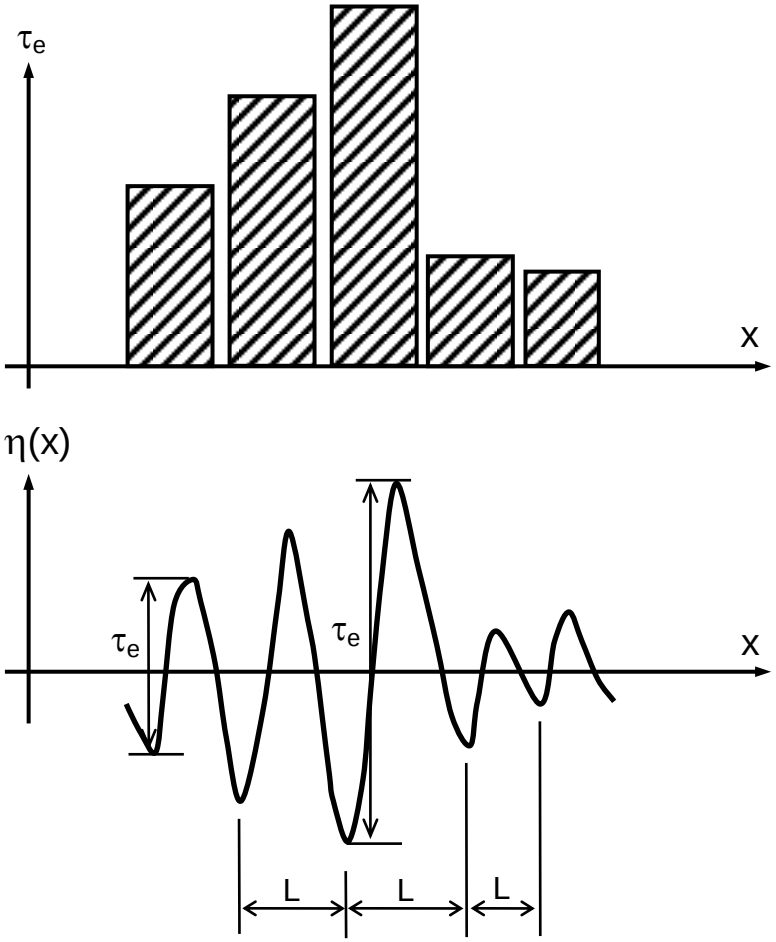

Fig. 8. Wave Process Generated Based on Effective Shear Stresses

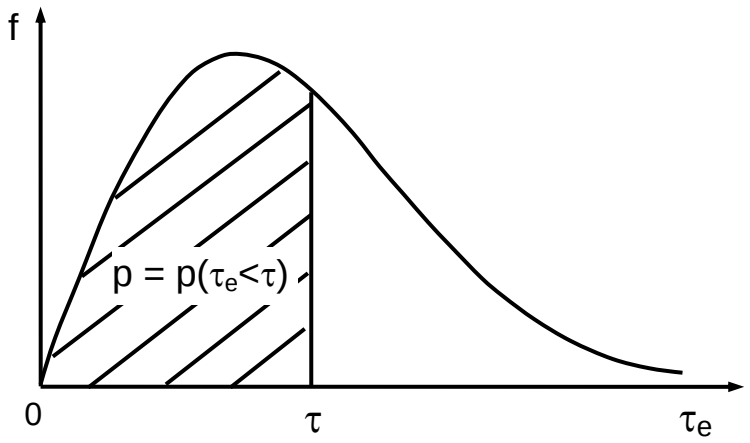

Fig. 9. Probability of Bed Particle Instability Defined Using Effective Shear Stress

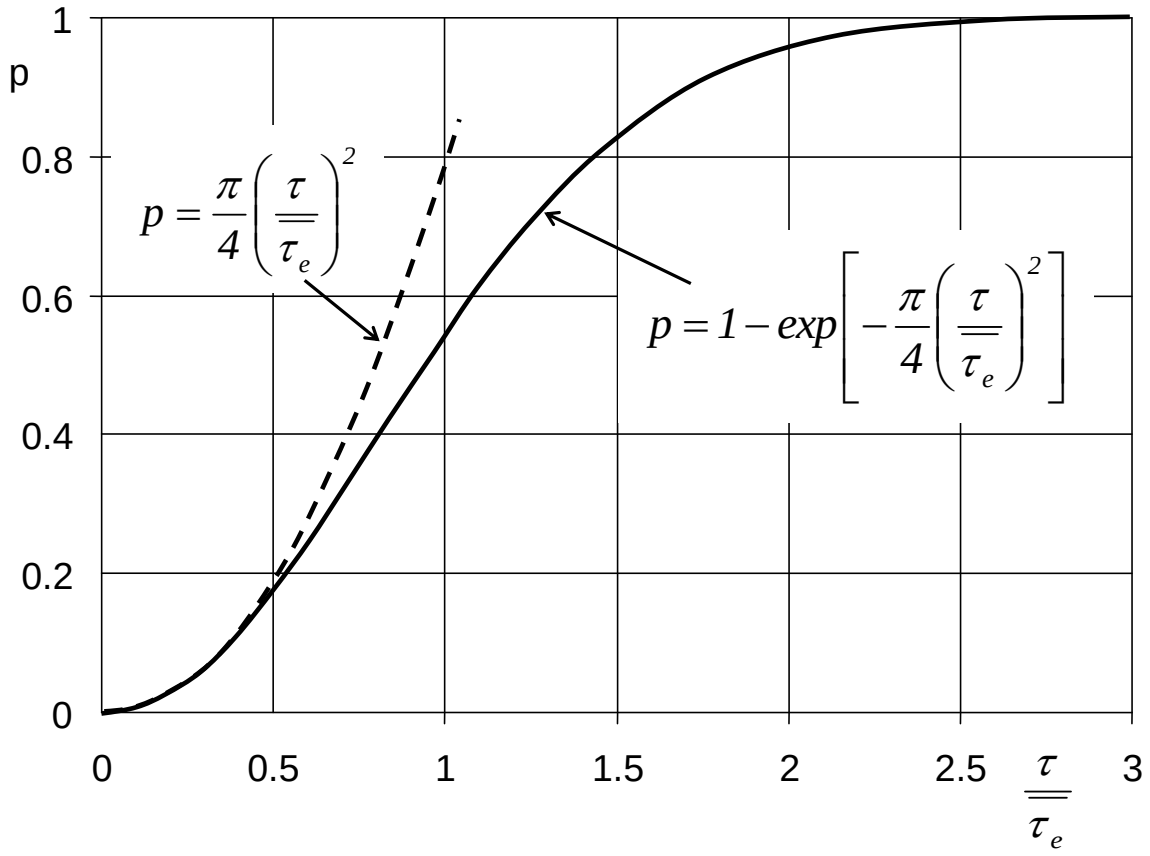

Fig. 10. Variation of Probability of Bed Particle Instability with Bed Shear Stress